

---

---

# Chapter 4

## The Hodgkin-Huxley Model

---

---

MARK NELSON and JOHN RINZEL

### 4.1 Introduction

Our present day understanding and methods of modeling neural excitability have been significantly influenced by the landmark work of Hodgkin and Huxley. In a series of five articles published in 1952 (Hodgkin, Huxley and Katz 1952, Hodgkin and Huxley 1952a–d) these investigators (together with Bernard Katz, who was a coauthor of the lead paper and a collaborator in several of the related studies) unveiled the key properties of the ionic conductances underlying the nerve action potential. For this outstanding achievement, Hodgkin and Huxley were awarded the 1963 Nobel Prize in Physiology and Medicine (shared with John Eccles, for his work on potentials and conductances at motoneuron synapses). The first four papers in the series summarize an experimental *tour de force* in which Hodgkin and Huxley brought to bear new experimental techniques for characterizing membrane properties. The final paper in the series places the experimental data into a comprehensive theoretical framework that forms the basis of our modern views of neural excitability. For a discussion and review of these seminal papers, see Rinzel (1990).

Hodgkin and Huxley indeed were aware that their findings and ideas had broad implications; they implicitly acknowledged this by the title of their fifth paper (Hodgkin and Huxley 1952d), which was the only one in the series not to explicitly mention the squid by name. Although the squid giant axon ultimately may have served as a means to an end, this is not to deny the squid her proper credit. Her generosity in providing a technically convenient preparation — a gargantuan axon, up to 1 *mm* in diameter — is often acknowledged. Less

widely appreciated is the fortuitous fact that, relative to most excitable nerve membrane, the squid axon is a simple system with basically only two types of voltage-dependent conductances. Today, we know of many more conductance types that can contribute to the excitability of nerve cells (Llinás 1988; also, see Chapter 7 in this volume). The squid axon membrane was an ideal model system; it presented a suitably generic and tractable problem, the solution of which gave rise to powerful new techniques and fundamental concepts.

In this chapter, we explore the Hodgkin-Huxley (HH) model using a GENESIS tutorial simulation called *Squid*. Before describing the mathematical model and performing the simulations, we provide a brief historical overview, so that the reader may better appreciate the scientific impact this work had at the time and how it has come to shape our present understanding of neural excitability. In exploring the HH model in this chapter, we will only be able to touch on some of the highlights. For a fuller appreciation of the model, we recommend a careful reading of the original paper (Hodgkin and Huxley 1952d). Additional historical and biophysical background on the HH model may also be found in Cole (1968), Hodgkin (1976), and Hille (1984).

## 4.2 Historical Background

For perspective, we begin by recounting the experimental evidence and theoretical concepts about neural excitability that existed at the time when Hodgkin and Huxley were developing their ideas and techniques. At that time, it was known that nerve cells had a low-resistance cytoplasm surrounded by a high-resistance membrane, that the membrane had an associated electrical capacitance, and that there was an electrical potential difference between the inside and the outside of the cell. It is important to note that until about 1940, there was no way to measure the membrane potential directly. Prior to that time, observations of nerve cell activity were made only with extracellular electrodes, which are capable of detecting electrical activity and action potentials, but only provide indirect information about the membrane potential itself.

A key piece of experimental data on neural excitability was obtained when Cole and Curtis (1939) used a Wheatstone bridge circuit to obtain the first convincing evidence for a transient increase in membrane conductance during an action potential. Their results were generally consistent with a popular hypothesis proposed much earlier by Bernstein (1902) that predicted a massive increase in membrane permeability during an action potential. Bernstein had formulated his hypothesis by reasoning as follows. It was known that a cell's membrane separated solutions of different ionic concentrations, with a much higher concentration of potassium inside than outside, and the opposite for sodium. By applying Nernst's theory, Bernstein was led to suggest that the resting membrane was semipermeable only to potassium, implying that at rest the membrane potential  $V_m$  should be close to the potassium equilibrium potential  $E_K$  of about  $-75$  mV. Then, during activity, he believed

that a “breakdown” in the membrane’s resistance to all ionic fluxes would occur and the potential difference across the membrane should disappear; i.e.,  $V_m$  would tend to zero. Although the conductance increase observed by Cole and Curtis (1939) during the action potential was qualitatively consistent with Bernstein’s hypothesis, the increase was not as large as one would expect from an extensive membrane breakdown.

During a postdoctoral visit in the U. S. spanning 1937–38, Hodgkin established ties with Cole’s group at Columbia University and worked with them also at Woods Hole in the summer. He and Curtis almost succeeded in measuring  $V_m$  directly by tunneling along the giant axon with a glass micropipette (Fig. 4.1A). Eventually, both Hodgkin and Curtis succeeded in this endeavor, albeit with other collaborators (Curtis and Cole 1940, Hodgkin and Huxley 1939), and they found not only did  $V_m$  rise transiently toward zero, but surprisingly there was a substantial overshoot, such that the membrane potential actually reversed in sign at the peak of the action potential (Fig. 4.1B). This result brought into serious question Bernstein’s simple idea of membrane breakdown and provided much food for thought during the span of World War II when Hodgkin, Huxley, and many other scientists were involved in the war effort.

Further insights into the nature of the membrane changes that occurred during an action potential required the development of two important experimental techniques referred to as the *space clamp* and the *voltage clamp*. The space clamp technique was developed by Marmont (1949) and Cole (1949) as a means of maintaining a uniform spatial distribution of membrane voltage  $V_m$  over the region of the cell where one was attempting to measure the membrane current. This could not be accomplished using the intracellular capillary electrode technique that had been developed to directly measure membrane potentials (Curtis and Cole 1940, Hodgkin and Huxley 1939). The tip of the capillary electrode acted essentially as a point source of current that would flow intracellularly along the axon, away from the recording site and not just through the membrane near the electrode. To achieve space clamping, the axon was threaded with a silver wire to provide a very low axial resistance, thereby eliminating longitudinal voltage gradients.

In conjunction with the space clamp, Cole and colleagues were also developing the voltage clamp technique that would allow the membrane potential to be maintained at any desired voltage level. One might think this simply would be a matter of connecting a constant voltage source across the cell membrane using a pair of electrodes, one inside and one outside the cell. In practice, this simple approach doesn’t work particularly well because of unpredictable voltage drops that occur in the solutions surrounding the electrodes. The technique that was eventually developed involved two pairs of electrodes. One pair was used to monitor the voltage across the membrane and the other was used to inject enough current to keep the measured voltage constant. In order to keep pace with the rapid changes in membrane permeability, the injected “clamping current” was controlled using a feedback amplifier circuit (Fig. 4.2A).

In order to take full advantage of the space clamp and voltage clamp techniques, it

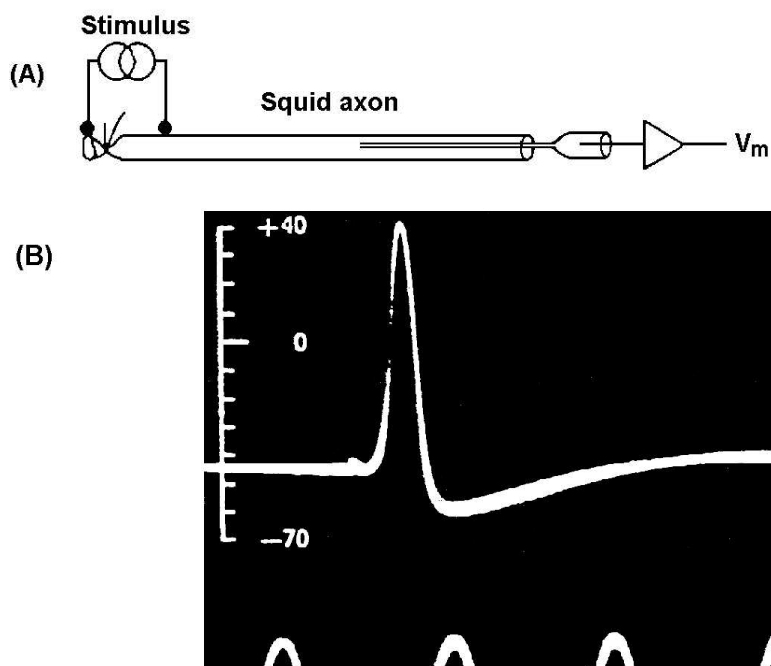


**Figure 4.1** First direct measurements of membrane potential in squid giant axon. (A) Capillary tube filled with sea water has been carefully pushed down axon and serves as electrode to measure potential difference across membrane (after Hille 1984). (B) Membrane voltage  $V_m$  (in  $mV$ ) during action potential. Time indicated by 500 Hz sine wave on oscilloscope screen. (Adapted from Hodgkin and Huxley (1939); reprinted with permission from *Nature*, Copyright 1939, Macmillan Magazines Limited.)

was necessary to develop a means for identifying the individual contributions to  $I_{ion}$  from different ion species. Work by Hodgkin and Katz (1949) had demonstrated that both sodium and potassium made important contributions to the ionic current. This work also helped explain the earlier puzzling observations that  $V_m$  overshoots zero during the action potential. In contrast to Bernstein, who imagined the action potential to result from an unbounded transient increase in permeability for all ions, Hodgkin and Katz realized that bounded changes in permeabilities for different ions could account for the observed changes in  $V_m$ . In their view,  $V_m$  would tend to the Nernst potential for the ion to which the membrane was dominantly permeable, and this dominance could change with time. For a membrane at rest, they agreed with Bernstein, that the potassium conductance is overriding, and hence the resting potential is near  $E_K$  (about  $-75 mV$ ). But during the action potential upstroke, they postulated that a dramatic shift took place, causing the membrane to become much more permeable to sodium than to potassium. Hence,  $V_m$  would tend toward  $E_{Na}$  (about  $+60 mV$ ), and an overshoot of zero potential would be expected. They predicted and showed, for

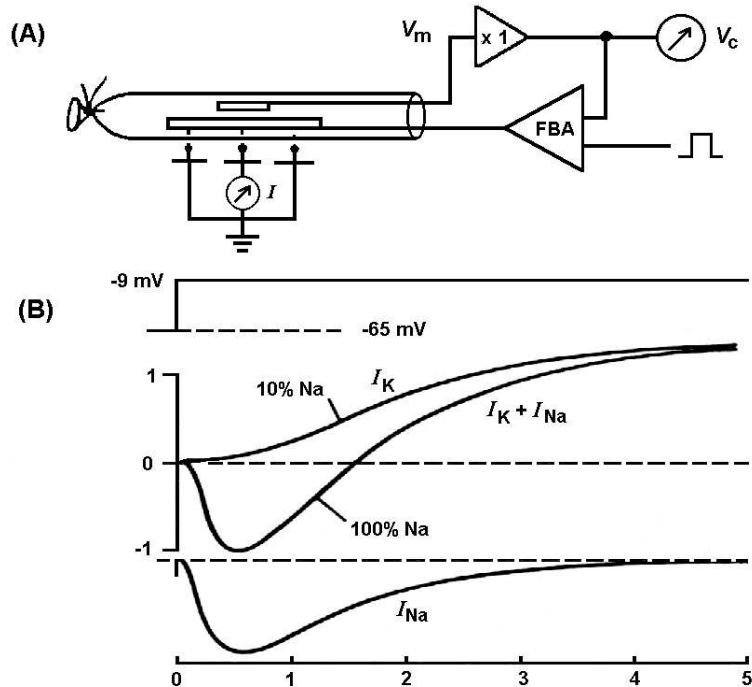


**Figure 4.2** Quantitative measurements of ionic currents in the squid giant axon using space clamp and voltage clamp techniques. (A) Schematic of setup. Axial wire to impose space clamp. Feedback amplifier for voltage clamp delivers current to maintain membrane potential  $V_m$  at command level  $V_c$  (adapted from Hille 1984). (B) Current ( $\text{mA}/\text{cm}^2$ ) versus time ( $\text{msec}$ ). Low sodium concentration in bath eliminates  $I_{Na}$ , so that  $I_K$  is recorded. Then subtraction from total current in normal sodium yields  $I_{Na}$ . Clamping voltage is  $-9 \text{ mV}$ , from a holding level of  $-65 \text{ mV}$ . (Replotted data from Hodgkin and Huxley (1952a).)

example, that the action potential amplitude depended critically on the concentration of external sodium; decreased sodium led to a lower peak for the action potential. In the theoretical section of their paper, they generalized the Nernst equation to predict the steady-state potential when the membrane is permeable with different degrees to more than one ionic species. This equation, modified from the earlier derivation by D. Goldman, is widely applied in cell biology, and is usually called the Goldman-Hodgkin-Katz equation.

The “sodium hypothesis” was a major conceptual advance. However, the question of how the permeability changes were dynamically linked to  $V_m$  was not completely addressed until the papers of 1952. Hodgkin and Huxley realized that by manipulating ionic concentrations in the axon and its environment, the contributions of different ionic conductances could be disentangled, provided that they responded independently to changes in  $V_m$  (a key assumption). By eliminating sodium from the bathing medium,  $I_{Na}$  becomes negligible and

so  $I_K$  is measured directly. Then  $I_{Na}$  can be determined by subtraction of  $I_K$  from the normal response as shown in Fig. 4.2B. Using this approach, Hodgkin and Huxley (1952b) were able to demonstrate convincingly that the current flowing across the squid axon membrane had only two major ionic components,  $I_{Na}$  and  $I_K$ , and that these currents were strongly influenced by  $V_m$ .

### 4.3 The Mathematical Model

Given this historical perspective, we can now better appreciate the insights provided by the HH model. In this section, we present the mathematical model itself. In subsequent sections we describe some of the experiments that Hodgkin and Huxley performed while developing their model, and we use GENESIS to simulate some of those experiments.

#### 4.3.1 Electrical Equivalent Circuit

The HH model is based on the idea that the electrical properties of a segment of nerve membrane can be modeled by an equivalent circuit of the form shown in Fig. 4.3. In the equivalent circuit, current flow across the membrane has two major components, one associated with charging the membrane capacitance and one associated with the movement of specific types of ions across the membrane. The ionic current is further subdivided into three distinct components, a sodium current  $I_{Na}$ , a potassium current  $I_K$ , and a small leakage current  $I_L$  that is primarily carried by chloride ions.

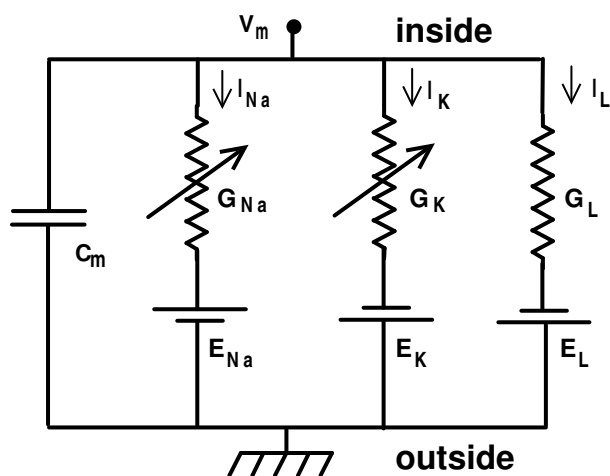


**Figure 4.3** Electrical equivalent circuit proposed by Hodgkin and Huxley for a short segment of squid giant axon. The variable resistances represent voltage-dependent conductances (Hodgkin and Huxley 1952d).

The behavior of an electrical circuit of the type shown in Fig. 4.3 can be described by a differential equation of the form:

$$C_m \frac{dV_m}{dt} + I_{ion} = I_{ext}, \quad (4.1)$$

where  $C_m$  is the membrane capacitance,  $V_m$  is the intracellular potential (membrane potential),  $I_{ion}$  is the net ionic current flowing across the membrane, and  $I_{ext}$  is an externally applied current.

### 4.3.2 HH Conventions

Note that the appearance of  $I_{ion}$  on the left-hand side of Eq. 4.1 and  $I_{ext}$  on the right indicates that they have opposite *sign conventions*. As the equation is written, a positive external current  $I_{ext}$  will tend to depolarize the cell (i.e., make  $V_m$  more positive) whereas a positive ionic current  $I_{ion}$  will tend to hyperpolarize the cell (i.e., make  $V_m$  more negative). This sign convention for ionic currents is sometimes referred to as the *physiologists' convention* and is summarized by the phrase “inward negative,” meaning that an inward flow of positive ions into the cell is considered a negative current. This convention perhaps arose from the fact that when one studies an ionic current in a voltage clamp experiment, rather than measuring the ionic current directly, one actually measures the clamp current that is necessary to counterbalance it. Thus an inward flow of positive ions is observed as a negative-going clamp current, hence explaining the “inward negative” convention. While reading later chapters, it will be important to realize that internally GENESIS uses the opposite sign convention (“inward positive”), since that allows all currents to be treated consistently, without making a special case for ionic currents. In the *Squid* tutorial in this chapter, however, currents are plotted using the physiologists' convention.

While we're on the topic of *conventions*, there are two more issues that should be discussed here. The first concerns the *value* of the membrane potential  $V_m$ . Recall that potentials are relative; only potential differences can be measured directly. Thus when defining the intracellular potential  $V_m$ , one is free to choose a convention that defines the resting intracellular potential to be zero (the convention used by Hodgkin and Huxley), *or* one could choose a convention that defines the extracellular potential to be zero, in which case the resting intracellular potential would be around  $-70$  mV. In either case the potential *difference* across the membrane is the same; it's simply a matter of how “zero” is defined. GENESIS allows the user to choose any convention they like; in the *Squid* tutorial we use the HH convention that the resting membrane potential is zero.

The second convention we need to discuss concerns the *sign* of the membrane potential. The modern convention is that depolarization makes the membrane potential  $V_m$  more positive. However, Hodgkin and Huxley (1952d) use the opposite sign convention (depolarization negative) in their paper. In the *Squid* tutorial, we use the modern convention that

depolarization is positive. At a conceptual level, the choice of conventions for currents and potentials is inconsequential; however, at the implementation level it matters a great deal, since getting one of the signs wrong will cause the model to behave incorrectly. The most important thing in choosing conventions is to ensure that the choices are internally self-consistent. One must pay careful attention to these issues when implementing a GENESIS simulation using equations from a published model, since it may be necessary to convert the published equations into a form that is consistent with the rest of the simulation.

### 4.3.3 The Ionic Current

The total ionic current  $I_{ion}$  in Eq. 4.1 is the algebraic sum of the individual contributions from all participating ion types:

$$I_{ion} = \sum_k I_k = \sum_k G_k(V_m - E_k). \quad (4.2)$$

Each individual ionic component  $I_k$  has an associated conductance value  $G_k$  (conductance is the reciprocal of resistance,  $G_k = 1/R_k$ ) and an equilibrium potential  $E_k$  (the potential for which the net ionic current flowing across the membrane is zero). The current is assumed to be proportional to the conductance times the driving force, resulting in terms of the general form  $I_k = G_k(V_m - E_k)$ . In the HH model of the squid giant axon, there are three such terms: a sodium current  $I_{Na}$ , a potassium current  $I_K$ , and a leakage current  $I_L$ :

$$I_{ion} = G_{Na}(V_m - E_{Na}) + G_K(V_m - E_K) + G_L(V_m - E_L). \quad (4.3)$$

In order to explain their experimental data, Hodgkin and Huxley postulated that  $G_{Na}$  and  $G_K$  changed dynamically as a function of membrane voltage. Today, we know that the basis for this voltage-dependence can be traced to the biophysical properties of the membrane channels that control the flow of ions across the membrane. It is important to remember that at the time Hodgkin and Huxley developed their model, there was very little information available about the biophysical structure of membrane or the molecular events underlying neural excitability. The modern concept of ion-selective membrane channels controlling the flow of ions across the membrane was only one of several competing ideas at the time. An important accomplishment of the HH model was to rule out several of the alternative ideas that had been proposed concerning membrane excitability.

Although Hodgkin and Huxley did not know about membrane channels when they developed their model, it is convenient for us to describe the voltage-dependent aspects of their model in those terms. The macroscopic conductances  $G_k$  of the HH model can be thought of as arising from the combined effects of a large number of microscopic ion channels embedded in the membrane. Each individual ion channel can be thought of as containing a small number of physical *gates* that regulate the flow of ions through the channel. An individual gate can be in one of two states, *permissive* or *non-permissive*. When *all* of the gates



for a particular channel are in the permissive state, ions can pass through the channel and the channel is *open*. If any of the gates are in the non-permissive state, ions cannot flow and the channel is *closed*.<sup>1</sup>

The voltage-dependence of ionic conductances is incorporated into the HH model by assuming that the probability for an individual gate to be in the permissive or non-permissive state depends on the value of the membrane voltage. If we consider gates of a particular type  $i$ , we can define a probability  $p_i$ , ranging between 0 and 1, that represents the *probability* of an individual gate being in the permissive state. If we consider a large number of channels, rather than an individual channel, we can also interpret  $p_i$  as the *fraction* of gates in that population that are in the permissive state and  $(1 - p_i)$  as the fraction in the non-permissive state. Transitions between permissive and non-permissive states in the HH model are assumed to obey first-order kinetics:

$$\frac{dp_i}{dt} = \alpha_i(V) (1 - p_i) - \beta_i(V) p_i, \quad (4.4)$$

where  $\alpha_i$  and  $\beta_i$  are voltage-dependent *rate constants* describing the “non-permissive to permissive” and “permissive to non-permissive” transition rates, respectively. If the membrane voltage  $V_m$  is “clamped” at some fixed value  $V$ , then the fraction of gates in the permissive state will eventually reach a steady-state value (i.e.,  $dp_i/dt = 0$ ) as  $t \rightarrow \infty$  given by:

$$p_{i,t \rightarrow \infty}(V) = \frac{\alpha_i(V)}{\alpha_i(V) + \beta_i(V)}. \quad (4.5)$$

The time course for approaching this equilibrium value is described by a simple exponential with time constant  $\tau_i(V)$  given by:

$$\tau_i(V) = \frac{1}{\alpha_i(V) + \beta_i(V)}. \quad (4.6)$$

When an individual channel is open (i.e., when all the gates are in the permissive state), it contributes some small, fixed value to the total conductance and zero otherwise. The macroscopic conductance for a large population of channels is thus proportional to the number of channels in the open state which is, in turn, proportional to the probability that the associated gates are in their permissive state. Thus the macroscopic conductance  $G_k$  due to channels of type  $k$ , with constituent gates of type  $i$ , is proportional to the *product* of the individual gate probabilities  $p_i$ :

$$G_k = \bar{g}_k \prod_i p_i, \quad (4.7)$$

---

<sup>1</sup>Although it would seem natural to speak of *gates* as being *open* or *closed*, a great deal of confusion can be avoided by consistently using the terminology *permissive* and *non-permissive* for *gates* while reserving the terms *open* and *closed* for *channels*.

where  $\bar{g}_k$  is a normalization constant that determines the maximum possible conductance when all the channels are open.

We have presented Eqs. 4.4–4.7 using a generalized notation that can be applied to a wide variety of conductances beyond those found in the squid axon. To conform to the standard notation of the HH model, the probability variable  $p_i$  in Eqs. 4.4–4.6 is replaced by a convenient notation in which the variable name is the same as the gate type. For example, Hodgkin and Huxley modeled the sodium conductance using three gates of a type labeled  $m$  and one gate of type  $h$ . Applying Eq. 4.7 to the sodium channel using both the generalized notation and the standard notation yields:

$$G_{Na} = \bar{g}_{Na} p_m^3 p_h \equiv \bar{g}_{Na} m^3 h. \quad (4.8)$$

Similarly, the potassium conductance is modeled with four identical “ $n$ ” gates:

$$G_K = \bar{g}_K p_n^4 \equiv \bar{g}_K n^4. \quad (4.9)$$

Summarizing the ionic currents in the HH model in standard notation, we have:

$$I_{ion} = \bar{g}_{Na} m^3 h (V_m - E_{Na}) + \bar{g}_K n^4 (V_m - E_K) + \bar{g}_L (V_m - E_L), \quad (4.10)$$

$$\frac{dm}{dt} = \alpha_m(V) (1 - m) - \beta_m(V) m, \quad (4.11)$$

$$\frac{dh}{dt} = \alpha_h(V) (1 - h) - \beta_h(V) h, \quad (4.12)$$

$$\frac{dn}{dt} = \alpha_n(V) (1 - n) - \beta_n(V) n. \quad (4.13)$$

The task that remains is to specify exactly how the six rate constants in Eqs. 4.11–4.13 depend on the membrane voltage. Then Eqs. 4.10–4.13, together with Eq. 4.1, completely specify the behavior of the membrane potential  $V_m$  in the model.

## 4.4 Voltage Clamp Experiments

How did Hodgkin and Huxley go about determining the voltage-dependence of the rate constants  $\alpha$  and  $\beta$  that appear in the kinetic equations Eqs. 4.11–4.13? How did they determine that the potassium conductance should be modeled with four identical  $n$  gates, but that the sodium conductance required three  $m$  gates and one  $h$  gate? In order to answer these questions, we need to look in some detail at the results of the voltage clamp experiments carried out by Hodgkin and Huxley.

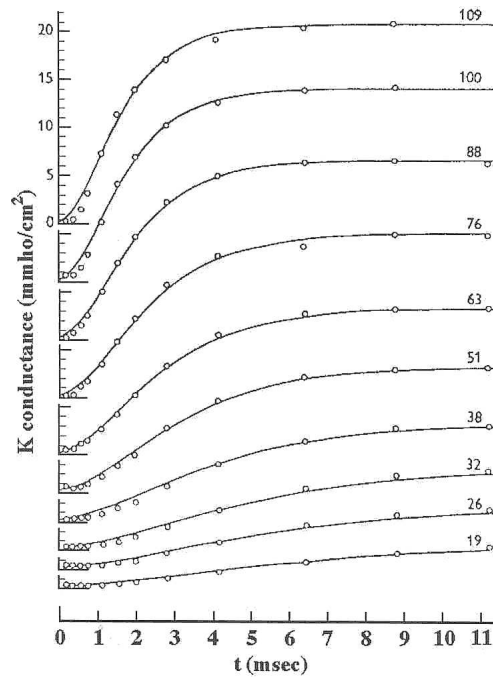


**Figure 4.4** Experimental voltage clamp data illustrating voltage-dependent properties of the potassium conductance in squid giant axon. Data points are shown as open circles. Solid lines are best-fit curves of the form given in Eq. 4.20. The command voltage  $V_c$  ( $mV$ ) is shown on the right-hand side of each curve. Redrawn from Hodgkin and Huxley (1952d).

#### 4.4.1 Characterizing the K Conductance

Figure 4.4 shows some voltage clamp results obtained by Hodgkin and Huxley in which the time course of the potassium conductance is plotted for several different values of the command voltage. The most obvious trend in the data is that the steady-state K conductance level increases with increasing command voltage. A second, somewhat more subtle trend is that the rising phase of the conductance change becomes more rapid with increasing depolarization. For small depolarizations on the order of  $20\text{ mV}$ , the half-maximum point occurs about  $5\text{ msec}$  after the onset of the change in voltage, whereas for large depolarizations on the order of  $100\text{ mV}$ , the half-maximum point is reached in about  $2\text{ msec}$ .

Hodgkin and Huxley incorporated these voltage-dependent properties of the K conductance into a mathematical model by first writing down an equation that describes the time evolution of a first-order kinetic process:

$$\frac{dn}{dt} = \alpha_n(V) (1 - n) - \beta_n(V) n. \quad (4.14)$$

In the experiments illustrated in Fig. 4.4, the membrane potential starts in the resting state ( $V_m = 0$ ) and is then instantaneously stepped to a new clamp voltage  $V_c$ . What is the time course of the state variable  $n$  under these circumstances? Initially, with  $V_m = 0$ , the state variable  $n$  has a resting value given by Eq. 4.5,

$$n_\infty(0) = \frac{\alpha_n(0)}{\alpha_n(0) + \beta_n(0)}. \quad (4.15)$$

When  $V_m$  is clamped to  $V_c$ ,  $n$  will eventually reach a steady-state value given by

$$n_\infty(V_c) = \frac{\alpha_n(V_c)}{\alpha_n(V_c) + \beta_n(V_c)}. \quad (4.16)$$

The solution to Eq. 4.14 that satisfies these boundary conditions is a simple exponential of the form

$$n(t) = n_\infty(V_c) - (n_\infty(V_c) - n_\infty(0))e^{-t/\tau_n}, \quad (4.17)$$

where

$$\tau_n(V_c) = \frac{1}{\alpha_n(V_c) + \beta_n(V_c)}. \quad (4.18)$$

Given Eq. 4.17, which describes the time course of  $n$  in response to a step change in command voltage, one could try fitting curves of this form to the conductance data shown in Fig. 4.4 by finding values of  $n_\infty(0)$ ,  $n_\infty(V_c)$ , and  $\tau_n(V_c)$  that give the best fit to the data for each value of  $V_c$ . Figure 4.5 illustrates this process, using some simulated conductance data generated by the Hodgkin-Huxley model. Recall that  $n$  takes on values between 0 and 1, so in order to fit the conductance data,  $n$  must be multiplied by a normalization constant  $\bar{g}_K$  that has units of conductance. For simplicity, the normalized conductance  $G_k/\bar{g}_K$  is plotted. The dotted line in Fig. 4.5 shows the best-fit results for a simple exponential curve of the form given in Eq. 4.17. Although this simple form does a reasonable job of capturing the general time course of the conductance change, it fails to reproduce the S-shaped (sigmoidal) trend in the data. This discrepancy is most apparent near the onset of the conductance change, shown in the inset of Fig. 4.5. Hodgkin and Huxley realized that a more sigmoidal time course could be generated if they considered the conductance to be proportional to a higher power of  $n$ . Figure 4.5 shows the results of fitting the conductance data using successively higher powers  $p$ . Using this sort of fitting procedure, Hodgkin and Huxley determined that a reasonable fit to their K conductance data could be obtained using a value of  $p = 4$ . Thus they arrived at a description for the K conductance given by

$$G_K = \bar{g}_K n^4, \quad (4.19)$$

in which case, the equation describing the conductance change and satisfying the appropriate boundary conditions is

$$G_K = \{(G_\infty(V_c))^{1/4} - ((G_\infty(V_c))^{1/4} - (G_\infty(0))^{1/4})e^{-t/\tau_n}\}^4, \quad (4.20)$$

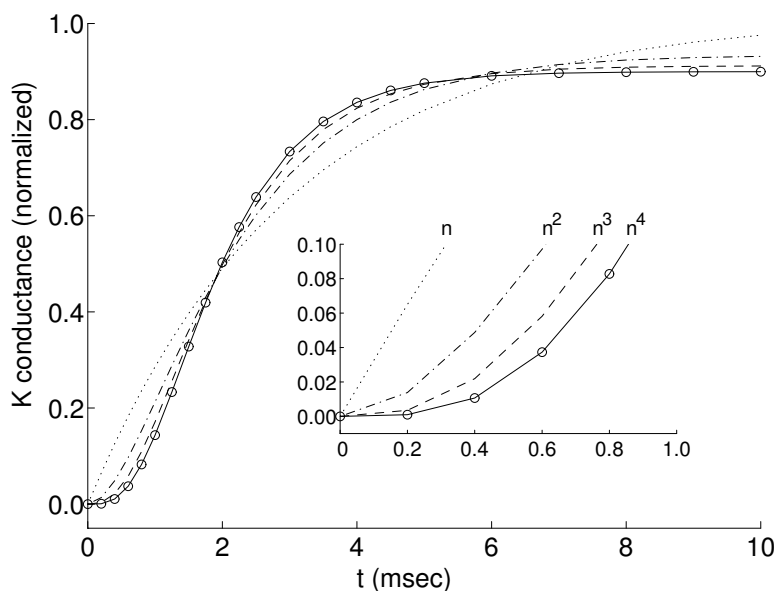


**Figure 4.5** Best-fit curves of the form  $G_k = \bar{g}_K n^p$  ( $p = 1-4$ ) for simulated conductance vs. time data (open circles). The inset shows an enlargement of the first millisecond of the response. The initial inflection in the curve cannot be well fit by a simple exponential (dotted line) that rises linearly from zero. Successively higher powers of  $p$  ( $p = 2$ : dot-dashed;  $p = 3$ : dashed line) result in a better fit to the initial inflection. In this case,  $p = 4$  (solid line) gives the best fit.

where  $G_\infty(0)$  is the initial conductance and  $G_\infty(V_c)$  is the steady-state conductance value attained when the command voltage is stepped to  $V_c$ . The solid lines in Fig. 4.4 show the best-fit results obtained by Hodgkin and Huxley for their data.

## 4.5 GENESIS: Voltage Clamp Experiments

In order to develop a better understanding of the procedures outlined above we will use the *Squid* tutorial to simulate a voltage clamp experiment of the type that Hodgkin and Huxley used to characterize the potassium conductance. Change to the *Scripts/squid* directory and start the *Squid* tutorial by typing “genesis Squid.” When the tutorial first loads, the simulation is in the current clamp mode. To switch to the voltage clamp mode, click the **Toggle Vclamp/Iclamp Mode** button. The first simulation experiment will be to hold the membrane potential at the resting potential for a couple of milliseconds (so we can see the baseline) and then rapidly clamp it to 50 mV above the resting potential. In this simulation, we measure voltages with respect to the resting potential, so we define the rest potential to be 0 volts, rather than  $-70$  mV.

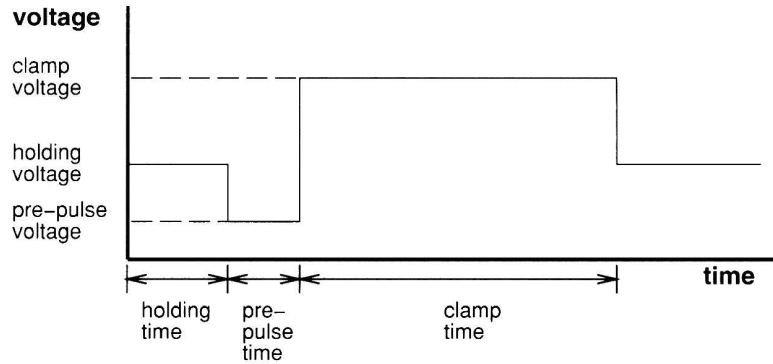


**Figure 4.6** The time course of the voltage clamp signal. These quantities can be set in the **Voltage Clamp Mode** control panel.

Figure 4.6 defines the quantities that are set by the **Voltage Clamp Mode** control panel. Make sure they are set to the following:

Holding Voltage	= 0 mV
Holding Time	= 2 msec
Pre-pulse Voltage	= 0 mV
Pre-pulse Time	= 0 msec
Clamp Voltage	= 50 mV
Clamp Time	= 20 msec

Now run the simulation by clicking **RESET** followed by **RUN**. Your display should look similar to that shown in Fig. 4.7. The plot at the upper left shows both the command voltage which is applied to the voltage clamp circuitry and the resulting membrane potential. If everything is working properly, these two curves should be almost identical, since the idea of the voltage clamp is that the membrane voltage should exactly follow the command voltage. The lower left plot shows the injection current (clamp current) used to maintain the desired voltage. The time course of the clamp current has three components: a very brief positive-going spike at the onset of the voltage change related to the charging of the membrane capacitance, a transient negative (inward) current associated with the sodium conductance, and finally a sustained positive (outward) current associated with the potassium conductance. The quantities shown in the two left panels are experimental observables and were accessible to Hodgkin and Huxley in their experiments, whereas the two right panels on your screen show quantities that are not directly observable (channel conductances and channel currents), but which we can plot in the simulation by “peeking” at the internal state of the model. In thinking about the data that Hodgkin and Huxley had to work with, keep in mind that the observables are confined to the two left panels.

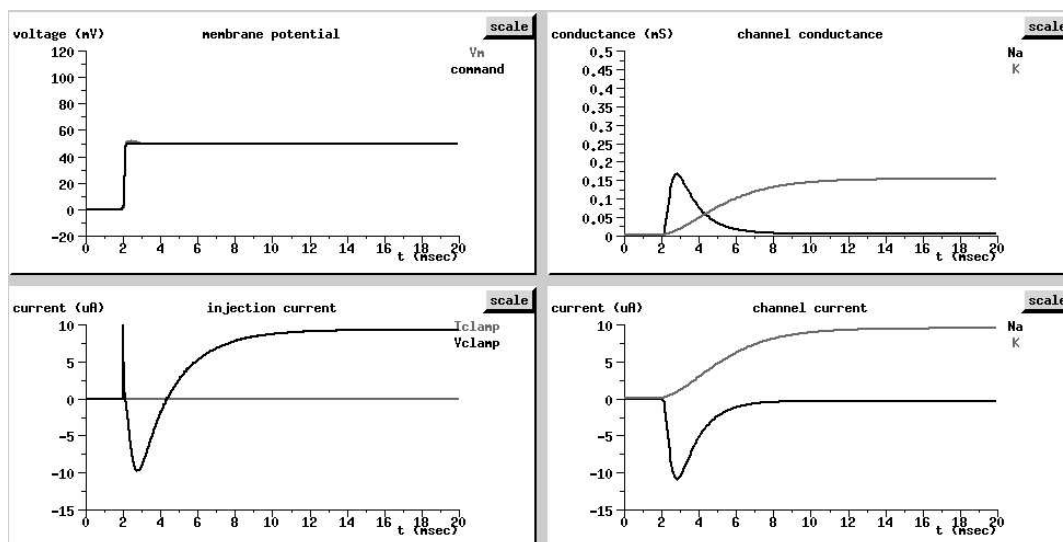


**Figure 4.7** A voltage clamp experiment using the *Squid* tutorial. Upper left: membrane voltage and clamp voltage; lower left: clamp current; upper right: Na and K channel conductances; lower right: Na and K channel currents.

In order to study the K conductance alone, Hodgkin and Huxley replaced Na in the external bathing solution with an impermeant ion, thus eliminating most of the Na contribution to the measured currents. We have an even easier way of getting rid of the sodium current in the simulation: click the toggle button labeled “Na channel unblocked,” so that it reads “Na channel blocked.” Now rerun the simulation. Note that the clamp current no longer shows the transient negative (inward) current associated with the Na conductance.

Now let’s do a voltage clamp series to characterize the K conductance. We’ll start with a large voltage step (so we can adjust graph scales) and work our way down through a series of smaller values. Change the **Clamp Voltage** dialog box value to 100 mV and rerun the simulation. (Don’t forget to hit “Return” after changing the contents of the dialog box!) Notice that values in some of the plots go off scale. To correct this situation, we can use the **scale** buttons in the upper left-hand corner of each display. For example, to adjust the scale for the clamp current, click the **scale** button on the lower left graph, set **y<sub>max</sub>** to 30, and then click **DONE**. If you want, you can adjust the scales of the other graphs in the same manner. Since we are going to perform a series of simulations and we want to see all the results plotted simultaneously, we’ll put the graphs into overlay mode (otherwise they get cleared on each reset). Click the toggle button labeled “**Overlay OFF**,” so that it reads “**Overlay ON**,” Now we’re ready to perform the next trial in the voltage series. Change the **Clamp Voltage** to 80 mV, click on **RESET**, and rerun the simulation. You should see the new data superimposed on the old data. Now continue the series with clamp voltages of 60,

40, and 20  $mV$ . When you are finished, the right side of your display should look similar to Fig. 4.8.

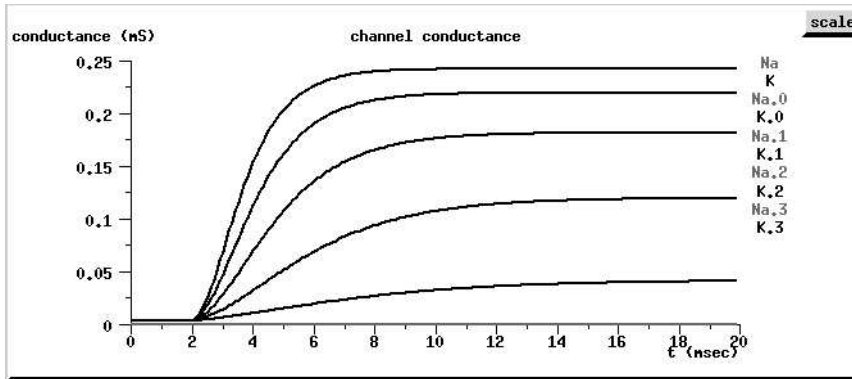


**Figure 4.8** Plots of K conductance vs. time for a simulated voltage clamp series with Na channels blocked. Responses are shown for five values of the clamp voltage: 20, 40, 60, 80 and 100  $mV$ . Compare with the experimental data in Fig. 4.4.

## 4.6 Parameterizing the Rate Constants

Using this procedure, Hodgkin and Huxley were able to determine the steady-state conductance values  $n_\infty(V_c)$  and time constants  $\tau_n(V_c)$  as a function of command voltage. Once values for  $n_\infty(V_c)$  and  $\tau_n(V_c)$  have been determined by fitting the conductance data, values for  $\alpha_n(V_c)$  and  $\beta_n(V_c)$  can be found from the following relationships:

$$\alpha_n(V) = \frac{n_\infty(V)}{\tau_n(V)} \quad (4.21)$$

$$\beta_n(V) = \frac{1 - n_\infty(V)}{\tau_n(V)}. \quad (4.22)$$

The open circles in Fig. 4.9 represent the experimentally determined values of  $n_\infty(V_c)$ ,  $\tau_n(V_c)$ ,  $\alpha_n(V_c)$ , and  $\beta_n(V_c)$  as a function of command voltage. Hodgkin and Huxley then found smooth curves that went through these data points. The empirically determined expressions for the rate constants  $\alpha_n$  and  $\beta_n$  are:

$$\alpha_n(V) = \frac{0.01(10 - V)}{\exp(\frac{10-V}{10}) - 1} \quad (4.23)$$

$$\beta_n(V) = 0.125 \exp(-V/80). \quad (4.24)$$



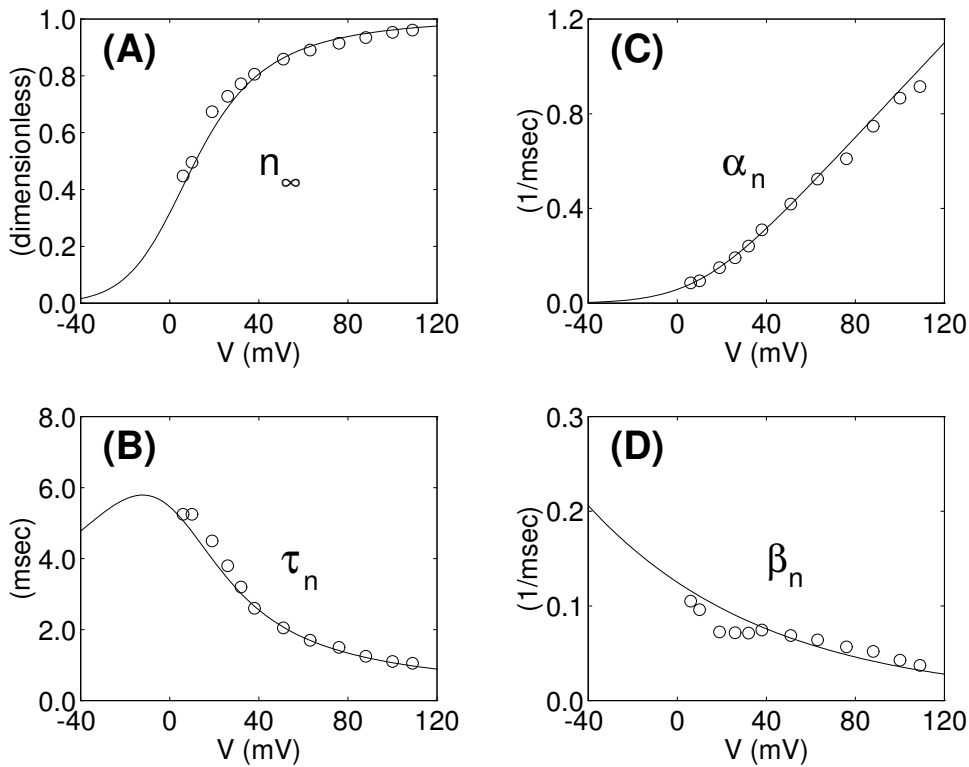


**Figure 4.9** Voltage dependence of K conductance parameters in the HH model. (A) Steady-state value  $n_{\infty}(V)$ ; (B) time constant  $\tau_n(V)$  (C) rate constant  $\alpha(V)$ ; and (D) rate constant  $\beta(V)$ . Open circles in (A) and (B) are best-fit parameters from voltage clamp data of the type shown in Fig. 4.4. Open circles in (C) and (D) are computed from Eqs. 4.21–4.22. Solid lines in (C) and (D) are empirical fits to the rate constant data of the form given in Eqs. 4.23–4.24. Solid lines in (A) and (B) are then calculated from Eqs. 4.16 and 4.18.

If you compare these expressions with Eqs. 12–13 in Hodgkin and Huxley (1952d), you will note that the sign of the membrane voltage has been changed to correspond to the modern convention (see Sec. 4.3.2).

## 4.7 Inactivation of the Na Conductance

There is an important qualitative difference between the Na and the K conductance changes that are observed in the squid axon under voltage clamp conditions. Namely, in response to a sustained voltage clamp step, the change in Na conductance is transient and only lasts a few milliseconds, whereas the change in K conductance is sustained and lasts as long as the voltage clamp is maintained. This effect can be seen in the upper right panel of Fig. 4.7.

To explore the Na conductance change in more detail, run the *Squid* simulation in voltage clamp mode with `Na channels unblocked` and `K channels blocked` (use the toggle buttons on the control form). Set the maximum simulation time to 10 msec in the Simulation Control panel and set the following values in the Voltage Clamp Mode control panel dialog boxes:

```

Holding Voltage   = 0 mV
Holding Time     = 2 msec
Pre-pulse Voltage = 0 mV
Pre-pulse Time   = 0 msec
Clamp Voltage    = 50 mV
Clamp Time       = 8 msec

```

Place the graphs in overlay mode (use the `Overlay ON` toggle button in the Simulation Control panel), and observe the magnitude and time course of the Na conductance change for clamp voltages between 10 and 70 mV. You will note that the magnitude of the peak conductance increases with increasing voltage and that the time constants of the rising and falling phases generally become shorter (faster) with increasing voltage.

In order to model these transient conductance changes, Hodgkin and Huxley needed to use a system of differential equations that was at least second-order. Using the same strategy as for the K conductance, they chose to do this by building up the higher-order response dynamics using a set of variables such that each obeys first-order kinetics. To describe the activation and inactivation phases of the Na conductance change requires two separate state variables, which Hodgkin and Huxley labeled  $m$  (the activation variable) and  $h$  (inactivation). In order to accurately capture the initial inflection in the conductance change, they found that they had to raise the  $m$  variable to the third power. Thus they arrived at a description for the Na conductance given by

$$G_{Na} = \bar{g}_{Na} m^3 h. \quad (4.25)$$

Following a procedure very similar to that outlined previously for the K conductance, Hodgkin and Huxley determined the voltage-dependence of the rate constants that govern the activation and inactivation variables. The empirically determined expressions that they arrived at for describing  $\alpha_m$ ,  $\beta_m$ ,  $\alpha_h$  and  $\beta_h$  are:

$$\alpha_m(V) = \frac{0.1(25 - V)}{\exp(\frac{25 - V}{10}) - 1}, \quad (4.26)$$

$$\beta_m(V) = 4 \exp(-V/18), \quad (4.27)$$

$$\alpha_h(V) = 0.07 \exp(-V/20), \quad (4.28)$$

$$\beta_h(V) = \frac{1}{\exp(\frac{30-V}{10}) + 1}. \quad (4.29)$$

Again, to be consistent with the modern sign convention used in GENESIS, we have flipped the sign of the voltage relative to the original Eqs. 20, 21, 23, 24 in Hodgkin and Huxley (1952d).

## 4.8 Current Injection Experiments

As we have seen, the form of the HH model and the values of the model parameters were all empirically determined from voltage clamp data. There was no *a priori* guarantee that the model would necessarily be successful in predicting the behavior of the squid axon under other experimental conditions. Thus it must have been extraordinarily satisfying for Hodgkin and Huxley to see their model produce realistic-looking action potentials when they numerically simulated the response to superthreshold current injections.

Run the *Squid* simulation in current clamp mode. Make sure that both the Na and K channels are unblocked. Set the maximum simulation time to 50 msec and set the following values in the Current Clamp Mode control panel:

```
Base Current      = 0.0 uA
Pulse Current 1   = 0.1 uA
Onset Delay 1     = 5.0 msec
Pulse Width 1    = 30.0 msec
Pulse Current 2   = 0.0 uA
Onset Delay 2     = 0.0 msec
Pulse Width 2    = 0.0 msec
Pulse Mode       = Single Pulse
```

With this set of parameters, you should observe a short train of action potentials in response to the injected current. Section 4.9 provides several suggested exercises for exploring properties of the HH model under current clamp conditions, including threshold behavior, refractory periods, depolarization block and anode break excitation.

## 4.9 Exercises

1. In voltage clamp mode, generate plots of peak conductance versus clamp voltage and peak current versus clamp voltage for the Na and K currents. (Characterize the Na and K components individually by using the appropriate toggle button to block the other component.) Select clamp voltages that cover the range from 40 mV below resting potential to 140 mV above resting potential. For each case, determine the

peak conductance and current from the graphs and use them in your plots. What is the general shape of the conductance vs. voltage plots? What is the general shape of the current vs. voltage plots? What are the reversal potentials for Na and K?

2. In voltage clamp mode, examine the effect of giving different hyperpolarizing pre-conditioning pulses prior to the voltage clamp step. (Suggested parameters: holding voltage = 0 mV; holding time = 5 msec; pre-pulse voltage = 0 to -50 mV in 10 mV steps; pre-pulse time = 5 msec; clamp voltage = +40 mV; clamp time = 20 msec.) What is the effect of the pre-conditioning pulse on the Na conductance? On the K conductance? In the context of the HH model, describe the mechanism responsible for this effect. How might this relate to the “after-hyperpolarization” that follows an action potential?
3. In current clamp mode, find the minimum current (threshold current) for eliciting a single action potential. (Suggested settings: base current = 0  $\mu$ A; onset delay 1 = 5 msec; pulse width 1 = 15 msec; simulation time = 20 msec.) How “sharp” is the threshold phenomenon — can you find a value of the injected current that gives a “half-height” action potential? If the threshold appears to be “all-or-none,” report the minimum fractional change in injection current that you tested (e.g., 1 part in 100, 1-in-1000, etc.).
4. The *rheobase* current is the minimum current that will elicit repetitive firing (i.e., generate a train of action potentials). What is the rheobase current for the *Squid* model? (Suggested settings: base current = 0  $\mu$ A; onset delay 1 = 5 msec; pulse width 1 = 95 msec; simulation time = 100 msec.) How sharp is the transition from single spike generation to repetitive firing? — Can you find a value of the injected current that generates *two* action potentials, but doesn’t fire repetitively?
5. By counting the number of spikes generated in a 100 msec window, construct a plot of firing frequency vs. injected current, starting at the rheobase current and working up to a value of about 10 times rheobase. (Suggested settings: base current = 0  $\mu$ A; onset delay 1 = 0 msec; pulse width 1 = 100 msec; simulation time = 100 msec.) How much does a 10-fold increase in injected current increase the firing rate? What happens if you increase the injected current to 100 times rheobase?
6. In problem 3 we saw that single action potentials can be elicited by small *sustained* levels of current injection. Single action potentials can also be elicited by *transient* pulses of current injection, even when the duration of the pulse is shorter than the duration of the action potential. As the length of the pulse decreases, however, the amplitude necessary to elicit an action potential increases. Generate a plot of single spike threshold current vs. pulse duration for pulse widths between 0.1 and 2.0 msec.

Is there a simple relationship between pulse width and threshold current? (Use an integration time step of 0.01 msec for this study.)

7. In this problem you will investigate the *refractory period* that follows each action potential. The *absolute* refractory period is the time interval during which no stimulus, regardless of strength, is capable of generating another action potential in the axon. The *relative* refractory period is the time interval during which a second action potential can be generated, but which requires an increased stimulus amplitude in order to do so. Using the two-pulse capability of the current clamp mode, map out the absolute and relative refractory periods of the model by generating a plot of threshold amplitude vs. latency. Use a pulse width of 1 msec. How long is the absolute refractory period? The relative refractory period? (When mapping out the absolute refractory period, make sure that the responses you call “spikes” are true “all-or-none” phenomena.)
8. All of the injection pulses in the previous current clamp problems have been depolarizing. In this problem you will look at the effect of hyperpolarizing current pulses. Set the pulse amplitude to  $-0.1 \mu A$  and set the pulse duration to 5 msec. What happens? What is the threshold, in terms of current magnitude and pulse duration, for eliciting this so-called *anode break* excitation? What mechanisms in the model are responsible for this behavior? (Hint: look at the time course of the state variables  $m$ ,  $n$  and  $h$ , using the `State Plot Visible` toggle button.)
9. Set the base current level just above rheobase to establish repetitive firing. Now superimpose a 1 msec duration,  $0.1 \mu A$  current pulse at various latencies ranging from 5.0 to 15.0 msec. Can you find a latency value that abolishes the repetitive firing?

